

Multiscale Atmospheric Dynamics: Cross-Frequency Phase-Amplitude Coupling in the Air Temperature

Milan Paluš*

Department of Nonlinear Dynamics and Complex Systems, Institute of Computer Science, Academy of Sciences of the Czech Republic, Pod vodárenskou věží 2, 182 07 Prague 8, Czech Republic

(Received 29 November 2012; published 21 February 2014)

Interactions between dynamics on different temporal scales of about a century long record of data of the daily mean surface air temperature from various European locations have been detected using a form of the conditional mutual information, statistically tested using the Fourier-transform and multifractal surrogate data methods. An information transfer from larger to smaller time scales has been observed as the influence of the phase of slow oscillatory phenomena with the periods around 6–11 yr on the amplitudes of the variability characterized by the smaller temporal scales from a few months to 4–5 yr. The overall effect of the slow oscillations on the interannual temperature variability within the range 1–2 °C has been observed in large areas of Europe.

DOI: [10.1103/PhysRevLett.112.078702](https://doi.org/10.1103/PhysRevLett.112.078702)

PACS numbers: 92.60.Ry, 05.45.Tp, 89.75.Da, 92.70.Gt

Understanding the complexity in the atmospheric dynamics and climate evolution is a great scientific challenge with a potentially high societal impact. Attempts to infer nonlinear dynamical mechanisms from meteorological data date back to the 1980s when a number of researchers claimed detections of a weather or climate attractor of a low dimension [1–3]. Other authors pointed to a limited reliability of chaos-identification algorithms and considered the observed low-dimensional weather or climate attractors as spurious [4,5]. Paluš and Novotná [6] even found the air temperature data well explained by a linear stochastic process, when the dependence between a temperature time series $\{x(t)\}$ and its lagged twin $\{x(t + \tau)\}$ was considered. Hlinka *et al.* [7] extended the latter result to the bivariate dependence of the monthly time series of the gridded whole-Earth air temperature reanalysis data.

On the other hand, a search for repetitive patterns on specific temporal scales in the temperature and other meteorological data has led to an identification of oscillatory phenomena possibly possessing a nonlinear origin and exhibiting phase synchronization between oscillatory modes extracted from either different types of climate-related data or data recorded at different locations on Earth [8–10]. Global circulation phenomena, identified as the principal modes of the atmospheric variability, also show a complex nonlinear behavior [11,12] and phase synchronization [13]. A different perspective in understanding the complexity of the atmospheric dynamics has been discovered by very active research in uncovering the long-term persistence and multifractality in climate-related time series including the air temperature [14–17].

Assuming that natural complex systems exhibit oscillations and fluctuations on a wide range of time scales, Gans *et al.* [18] propose a framework for analysis of

interactions across the temporal scales by quantifying dependence among instantaneous amplitudes and frequencies of oscillatory dynamics obtained from experimental time series using digital filters and the Hilbert transform. Cross-frequency interactions, in particular, a cross-frequency phase–amplitude coupling, has recently been observed in electrophysiological signals reflecting the brain dynamics. Beyond the synchronization phenomena on particular temporal scales, the cross-frequency coupling enriches the cooperative behavior of neuronal networks and apparently plays an important functional role in neuronal computation, communication, and learning [19].

It can generally be expected that long-term air temperature recordings reflect complex atmospheric dynamics on multiple temporal scales. Considering the oscillatory and synchronization phenomena observed on various scales of the atmospheric dynamics [8–10], in accord with Gans *et al.* [18], we will study in the air temperature recordings possible oscillations and fluctuations on a wide range of time scales using the phase dynamics approach [20]. For an arbitrary time series $s(t)$, the analytic signal $\psi(t)$ is a complex function of time defined as

$$\psi(t) = s(t) + i\hat{s}(t) = A(t)e^{i\phi(t)}. \quad (1)$$

The instantaneous phase $\phi(t)$ of the signal $s(t)$ is then

$$\phi(t) = \arctan \frac{\hat{s}(t)}{s(t)}, \quad (2)$$

and its instantaneous amplitude is

$$A(t) = \sqrt{s(t)^2 + \hat{s}(t)^2}. \quad (3)$$

The imaginary part $\hat{s}(t)$ of the analytic signal $\psi(t)$ is usually obtained by using the Hilbert transform of $s(t)$ [18,20]. Since the Hilbert transform is a unit gain filter at each frequency, broadband signals from multiscale processes should be prefiltered to the frequency band of interest. In this study, a continuous complex wavelet transform (CCWT) with the Morlet wavelet [21] is applied directly to experimental time series $s(t)$. At each time scale (frequency), the complex wavelet coefficients can be directly used in Eqs. (2) and (3) for the estimation of the phase $\phi(t)$ and the amplitude $A(t)$, respectively. The CCWT provides both the bandpass filtering of the signal and the estimation of the instantaneous phase and the instantaneous amplitude.

Let time series $\{x(t)\}$ and $\{y(t)\}$ be realizations of stationary, ergodic stochastic processes $\{X(t)\}$ and $\{Y(t)\}$. Information about the future X_τ of the process $\{X\}$, shifted τ time units forward, contained in the process $\{Y\}$ can be measured by the conditional mutual information (CMI) $I(Y; X_\tau | X)$, also known as the transfer entropy [22]. Paluš and Vejmelka [23] show that in the time series representation the functional $I(y(t); x(t+\tau) | x(t), x(t-\eta), \dots, x(t-m\eta))$ can be used for inference of causal (causality in the Granger sense [24]) influence of $\{Y\}$ on $\{X\}$. The conditioning variables depend on memory or dimensionality of the process $\{X\}$. Paluš and Stefanovska [25] demonstrate that the CMI can be applied to instantaneous phases of interacting oscillatory processes in order to detect the direction of coupling, i.e., to discern the driving from the driven system. Here, we study a possible influence of the phase ϕ_1 of slow oscillations on the amplitude A_2 of higher-frequency variability of the same multiscale process, using the functional

$$I(\phi_1(t); A_2(t+\tau) | A_2(t), A_2(t-\eta), \dots, A_2(t-m\eta)), \quad (4)$$

where τ is the forward time lag and η is the backward time lag in the $(m+1)$ -dimensional condition. For the statistical evaluation of the CMI (4), we use two types of surrogate data. Using the Fourier transform (FT) surrogate data [26] representing the null hypothesis of a linear stochastic process in which no interactions between different temporal scales exist, we perform just the randomization of the Fourier phases. No amplitude adjustment is done since in the next step the surrogate time series is processed by the CCWT and the exact preservation of the signal frequency content is our main interest. A more sophisticated null hypothesis is represented by the multifractal (MF) surrogate data [27] in which possible information transfer from larger to smaller scales, explained by random cascades on wavelet dyadic trees, is preserved.

In this study we use daily mean surface air temperature (SAT) time series recorded in various European locations: The data from Bamberg, Basel, De Bilt, Potsdam, Vienna, and Zurich from the period 1901–1999 are a part of the data compiled for the European Climate Assessment [28], the record from Prague-Klementinum is extended to 2008, and

the SAT data from a number of German stations extended to 2011 are available from the German Climate Data Center [29]. The inclusion criterion for this study is the availability of at least 90 yr of uninterrupted daily mean SAT recording, since the computations of the CMI (4) have been performed using the time series length 32768 daily samples. CMI estimators [24] suffer from bias and variance of various origins [23,30]. Therefore, the relatively large amount of data was required in order to obtain reliable estimates, even though we used an estimator of the mutual information derived for Gaussian processes [31–34]. For more details, see the Supplemental Material [35]. The functional (4) is evaluated and averaged for the forward lags τ from 1 to 750 days. The backward lag η is set to 1/4 of the period of the slower oscillations characterized by the phase ϕ_1 , following the embedding construction recipe based on the first minimum of the mutual information [36].

The temporal evolution of the raw daily mean SAT data from midlatitude locations is dominated by the annual cycle. In many climate-related studies deseasonalized SAT “anomalies” are used. In this study, however, we are interested in discovering interactions of all relevant temporal scales; therefore, the raw SAT data are used for the computation of the CMI (4). The surrogate data algorithms used, however, might not accurately reproduce such a strong cyclic component. The latter is not consistent with the multifractal model used [27], and even the FT surrogate data procedure fails to reproduce a strong cyclicality and/or long coherence times [37]. Therefore, before the randomization, the seasonality in both the mean and the variance is removed from each SAT time series. This is done by computing the means and the variances for each calendar day. These seasonal means are subtracted from the raw SAT data of the corresponding days, and the resultant SAT anomalies (SATA) are divided by the corresponding seasonal variances. Such deseasonalized data enter either the FT or the MF randomization procedure. Then, the original seasonality in variance and mean is added back to each surrogate data realization. Each “seasonalized” surrogate realization undergoes the same processing procedure as the original SAT data—the CCWT is used to obtain the phase ϕ_1 of slow oscillations and the amplitude A_2 of higher-frequency variability, both used in the CMI (4) estimation. For each pair of the studied temporal scales, 1000 surrogate realizations are used for an empirical estimation of the percentiles of the CMI (4) surrogate distribution. We record the highest percentile exceeded by the value of the CMI (4) computed from the original SAT data. This significance level is simply related to the statistical significance of a single statistical test: the significance level equal to 0.99 means that the CMI value is significantly greater than zero with $p < 0.01$. The two randomization procedures used give consistent results. Further details on the statistical evaluation are given in the Supplemental Material [35].

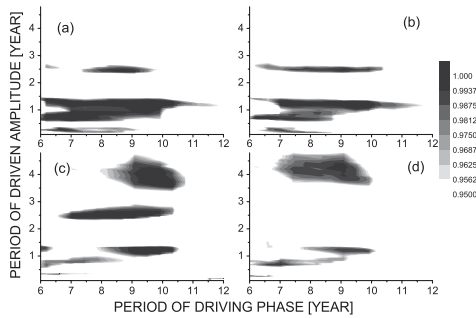


FIG. 1. Causal influence of the phase of slower oscillations on the amplitude of faster fluctuations in the daily surface air temperature from (a) Potsdam, (b) Hamburg, (c) Vienna, and (d) De Bilt. The significance levels for the conditional mutual information (4) with the three-dimensional condition, obtained using the Fourier-transform surrogate data, are coded in gray if they are greater than 0.95.

The significance levels for the CMI (4) computed using the SAT from four European locations are presented in Fig. 1. In the SAT from the Central European locations around and northward from 50°N [e.g., in Potsdam [Fig. 1(a)], or Prague [35]], and also more in the northwest direction, e.g., in the SAT from Hamburg [Fig. 1(b)], the oscillatory processes with the periods between 6 and 11 yr influence the variability on the time scales between 2 and 3 yr, around 3–4 months, and, at the largest extent, at and around the annual cycle. The pattern changes in the locations more to the south, e.g., in Vienna [Fig. 1(c)], or more to the west, close to the Netherland coast [De Bilt, Fig. 1(d)]. In the latter two cases, a decrease of the involvement of the driven variability on the scales close to the annual cycle is observed, accompanied by emergence of the driven variability on the time scales around 4–5 yr. A more detailed look at the significance levels for the patterns of the directional ϕ_1 – A_2 interactions for the A_2 periods around the annual cycle is presented in Fig. 2(a) for the SAT data from the Prague-Klementinum station. Here, as well as in Fig. 1, we present quantitative evidence that these slow (time scale 6–11 yr) phenomena influence the variability on the shorter time scales. Yet, this quantitative evidence for the causal cross-scale interactions does not give an estimate of the size of the effect. Let us evaluate the conditional means (CM) of the amplitude A_2 taken conditionally on the present value of the phase ϕ_1 using eight bins in the interval $(-\pi, \pi)$. Then, in Fig. 2(b) for the Prague SATA we plot the difference between the maximum and minimum values of the eight A_2 CMs in the eight phase bins within the cycle of ϕ_1 . This difference reflects a “strength” of the dependence of $A_2(t)$ on $\phi_1(t)$. However, due to the redundant character of the CCWT decomposition, these differences for different time scales give only a relative quantification of the change of the amplitude A_2 of

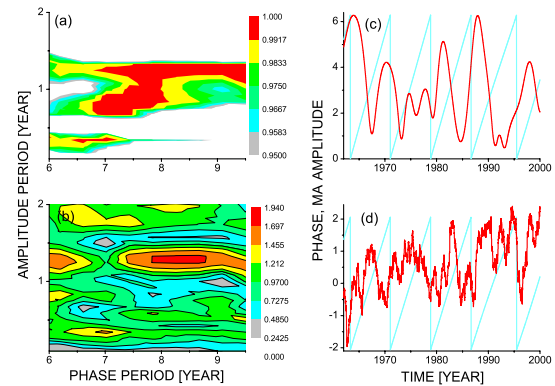


FIG. 2 (color online). (a) Causal influence (significance levels are color coded if they are greater than 0.95) of the phase of slower oscillations on the amplitude of faster fluctuations in the daily surface air temperature. (b) Differences (relative values) of the maximum and minimum conditional means of the amplitude A_2 (periods on the ordinate), conditioned on the phase ϕ_1 (periods on the abscissa). (c) The (CCWT-extracted) phase of the 8-yr cycle [light (blue) line, rad] and the moving averages of the amplitude [dark (red) curve, arbitrary units] of the 1.3-yr cycle. (d) The (CCWT-extracted) phase of the 8-yr cycle [light (blue) line, rescaled values] and the moving averages of the total SATA variability [dark (red) curve, $^\circ\text{C}$]. The Prague-Klementinum SAT data were analyzed, and the MAs were computed in a 1-yr moving window.

the fast variability within the slow cycle characterized by the phase ϕ_1 .

We can see in Fig. 2(b) that the strongest effect is exerted by the phase of the oscillations with the period around 8 yr on the variability characterized by the period approximately 1.3 yr. In order to see the evolution of ϕ_1 and A_2 in time, in Fig. 2(c) we plot the phase of the 8-yr cycle [lighter (blue) sawtooth lines, in each cycle rising from zero to 2π rad] and the relative values of the moving average (MA) of A_2 for the period 1.3 yr. We can see the tendency of A_2 to reach higher values in the first half of each 8-yr cycle (ϕ_1 between 0 and π) than in the second half of the cycle (ϕ_1 between π and 2π). In order to see the effect of the phase ϕ_1 on the temperature variability in a real physical quantity ($^\circ\text{C}$), the MA values for the total SATA variability together with the phase of the 8-yr cycle are plotted in Fig. 2(d). In all cycles (except the cycle in the years 1986–1995) the SATA variability reaches the maxima around the middle of the 8-yr cycle.

Oscillatory phenomena with the periods between 6 and 11 yr, however, most frequently with the period around 7–8 yr, have been observed in the air temperature and other meteorological data by many authors (see Ref. [10] and references therein). Recalling the study of Paluš and Novotná [8,10], in Fig. 3(a) we present a histogram of the instantaneous periods of an oscillatory mode extracted from the Prague SAT using the singular spectrum analysis [8]. The period of this oscillatory phenomenon fluctuates in

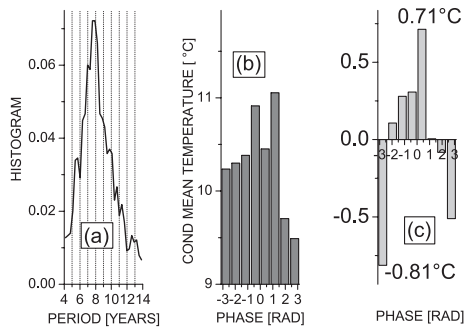


FIG. 3. (a) Histogram of instantaneous periods of the oscillatory mode extracted from the Prague-Klementinum SAT using the singular spectrum decomposition. (b) Conditional means of the Prague-Klementinum SAT, and (c) conditional means of the Prague-Klementinum SAT anomalies, computed conditionally on the phase of the SAT oscillatory mode extracted using the CCWT with the central wavelet period 8 yr.

a wide range; however, the most frequent period is close to 8 yr. Considering this observation and the results in Fig. 2(b), we use the CCWT in order to extract the instantaneous phase of the oscillatory mode with the central wavelet period 8 yr. Again, using eight bins in the interval $(-\pi, \pi)$, we evaluate the conditional SAT means taken conditionally on this phase. The maximum difference of the SAT conditional means within the 8-yr cycle is 1.56°C [Fig. 3(b)]. In order to remove the influence of the annual cycle itself, we repeat the computations for the SAT anomalies. The SATA CMs in Fig. 3(c) make the effect of the 8-yr cycle on the SATA variability, observed in Fig. 2(d), even more visible: The minimum SATA CM, -0.81°C , is located in the first bin and the maximum 0.71°C in the fifth of the eight bins covering the interval $(-\pi, \pi)$. The maximum SATA CM difference within the 8-yr cycle is equal to 1.52°C . These differences were obtained from the SAT and SATA Prague data in the period 1958–2003 (16 384 daily samples starting from Jan. 1, 1958) due to a comparability with the results from the gridded reanalysis data from the European Centre for Medium-Range Weather Forecasts. The ERA SATA, obtained as a concatenation of the ERA-40 and ERA-Interim data sets [38] on a regular $2.5^\circ \times 2.5^\circ$ grid over Europe, underwent the same conditional mean analysis using the phase of the CCWT-extracted 8-yr cycle. The maximum differences of the conditional SATA means within the 8-yr cycle, which are statistically significant (i.e., exceeding the MF surrogate mean by more than 2.4 standard deviations), are coded in gray in Fig. 4. Consistent with the station data, the ERA data suggest that the 8-yr cycle explains the interannual temperature variability in the range 1.5°C in the marked areas of the Czech Republic, Germany, and Poland, as well as in parts of other European countries. In some areas of Germany and Poland, this value reaches 2°C .

We have presented, for the first time, quantitative evidence for the information transfer from larger to smaller

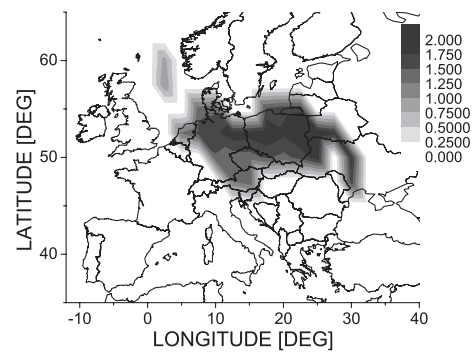


FIG. 4. Significant maximum differences of the conditional means of the ERA SAT anomalies (coded in gray, $^\circ\text{C}$) in relation to the phase of the SAT oscillatory mode extracted using the CCWT with the central wavelet period 8 yr.

time scales in the atmospheric dynamics. The information transfer has been observed in the surface air temperature daily mean time series as the causal influence of the phase of slow oscillatory phenomena with the periods around 6–11 yr on the amplitudes of the variability characterized by the smaller temporal scales from a few months to 4–5 yr. We hypothesize that the observed phenomenon might stem from local effects of the North Atlantic Oscillation, one of the global modes of the atmospheric circulation variability [35]. Chekroun *et al.* [39] observed that the phase of the low-frequency variability of the El Niño—Southern Oscillation determines the character of high-frequency variability (“weather noise”) of the sea-surface temperature in the tropical Pacific. In this study we have probably observed a regional manifestation of a general phenomenon of cross-scale interactions in the atmospheric dynamics in which global, low-frequency modes influence local, high-frequency variability. This phenomenon requires further study and understanding of its mechanism and deserves considerable attention in the evaluation of recent climate changes, at least on a regional level, since the overall effect of the slow oscillations on the interannual temperature variability within the range $1\text{--}2^\circ\text{C}$ has been observed in large areas of (mainly Central) Europe.

This study was supported by the Czech Science Foundation, Project No. P103/11/J068.

*mp@cs.cas.cz; <http://www.cs.cas.cz/mp/>

- [1] C. Nicolis and G. Nicolis, *Nature (London)* **311**, 529 (1984); **326**, 523 (1987).
- [2] K. Fraedrich, *J. Atmos. Sci.* **44**, 722 (1987).
- [3] A. A. Tsonis and J. B. Elsner, *Nature (London)* **333**, 545 (1988).
- [4] P. Grassberger, *Nature (London)* **323**, 609 (1986); **326**, 524 (1987).
- [5] E. N. Lorenz, *Nature (London)* **353**, 241 (1991).
- [6] M. Paluš and D. Novotná, *Phys. Lett. A* **193**, 67 (1994).

- [7] J. Hlinka, D. Hartman, M. Vejmelka, D. Novotná, and M. Paluš, *Clim. Dynam.*, doi: 10.1007/s00382-013-1780-2 (2013).
- [8] M. Paluš and D. Novotná, *Nonlinear Proc. Geophys.* **11**, 721 (2004); **13**, 287 (2006).
- [9] Y. Feliks, M. Ghil, and A. W. Robertson, *J. Clim.* **23**, 4060 (2010).
- [10] M. Paluš and D. Novotná, *J. Atmos. Sol. Terr. Phys.* **71** 923 (2009); *Nonlinear Proc. Geophys.* **18**, 251 (2011).
- [11] J. Boucharel, B. Dewitte, Y. Penhoat, B. Garel, S.-W. Yeh, and J.-S. Kug, *Climate Dynamics* **37**, 2045 (2011).
- [12] S. M. Osprey and M. H. P. Ambaum, *Geophys. Res. Lett.* **38**, L15702 (2011).
- [13] K. Stein, A. Timmermann, and N. Schneider, *Phys. Rev. Lett.* **107**, 128501 (2011).
- [14] E. Koscielny-Bunde, A. Bunde, S. Havlin, H. Roman, Y. Goldreich, and H.-J. Schellnhuber, *Phys. Rev. Lett.* **81**, 729 (1998).
- [15] J. F. Eichner, E. Koscielny-Bunde, A. Bunde, S. Havlin, and H. J. Schellnhuber, *Phys. Rev. E* **68**, 046133 (2003).
- [16] J. W. Kantelhardt, E. Koscielny-Bunde, D. Rybski, P. Braun, A. Bunde, and S. Havlin, *J. Geophys. Res.* **111**, D01106 (2006).
- [17] J. Alvarez-Ramirez, J. Alvarez, L. Dagdug, E. Rodriguez, and J. C. Echeverria, *Physica (Amsterdam)* **387A**, 3629 (2008).
- [18] F. Gans, A. Y. Schumann, J. W. Kantelhardt, T. Penzel, and I. Fietze, *Phys. Rev. Lett.* **102**, 098701 (2009).
- [19] R. Canolty and R. T. Knight, *Trends Cognit. Sci.* **14**, 506 (2010).
- [20] A. Pikovsky, M. Rosenblum, and J. Kurths, *Synchronization. A Universal Concept in Nonlinear Sciences* (Cambridge University Press, Cambridge, England, 2001).
- [21] C. Torrence and G. P. Compo, *Bull. Am. Meteorol. Soc.* **79**, 61 (1998).
- [22] T. Schreiber, *Phys. Rev. Lett.* **85**, 461 (2000).
- [23] M. Paluš and M. Vejmelka, *Phys. Rev. E* **75**, 056211 (2007).
- [24] K. Hlaváčková-Schindler, M. Paluš, M. Vejmelka, and J. Bhattacharya, *Phys. Rep.* **441**, 1 (2007).
- [25] M. Paluš and A. Stefanovska, *Phys. Rev. E* **67**, 055201R (2003).
- [26] J. Theiler, S. Eubank, A. Longtin, B. Galdrikian, and J. D. Farmer, *Physica (Amsterdam)* **58D**, 77 (1992); D. Prichard and J. Theiler, *Phys. Rev. Lett.* **73**, 951 (1994).
- [27] M. Paluš, *Phys. Rev. Lett.* **101**, 134101 (2008).
- [28] A. M. G. Klein Tank, J. B. Wijngaard, G. P. Können *et al.*, *Int. J. Climatol.* **22** 1441 (2002).
- [29] Deutscher Wetterdienst of the German Federal Ministry of Transport, Building and Urban Development, <http://www.dwd.de/>
- [30] M. Vejmelka and M. Paluš, *Phys. Rev. E* **77**, 026214 (2008).
- [31] M. Paluš, V. Albrecht, and I. Dvořák, *Phys. Lett. A* **175**, 203 (1993).
- [32] D. Prichard and J. Theiler, *Physica (Amsterdam)* **84D**, 476 (1995).
- [33] M. Paluš, *Phys. Lett. A* **213**, 138 (1996).
- [34] A. Molini, G. G. Katul, and A. Porporato, *J. Geophys. Res.* **115**, D14123 (2010).
- [35] See Supplemental Material at <http://link.aps.org/supplemental/10.1103/PhysRevLett.112.078702> for details.
- [36] A. M. Fraser and H. L. Swinney, *Phys. Rev. A* **33**, 1134 (1986).
- [37] M. Paluš, *Physica (Amsterdam)* **80D**, 186 (1995).
- [38] S. M. Uppala *et al.*, *Q. J. R. Meteorol. Soc.* **131**, 2961 (2005); D. P. Dee *et al.*, *Q. J. R. Meteorol. Soc.* **137**, 553 (2011).
- [39] M. D. Chekroun, D. Kondrashov, and M. Ghil, *Proc. Natl. Acad. Sci. U.S.A.* **108**, 11766 (2011).